Earth and Planetary Science Letters 607 (2023) 118068

Contents lists available at ScienceDirect

Earth and Planetary Science Letters

journal homepage: www.elsevier.com/locate/epsl

Resolving the fate of trace metals during microbial remineralization of phytoplankton biomass in precursor banded iron formation sediments

Kathryn I. Rico [a], Manuel Schad [b,c], Aude Picard [d], Andreas Kappler [b,e], Kurt O. Konhauser [c], Nagissa Mahmoudi [a,*]

[a] Department of Earth and Planetary Sciences, McGill University, 3450 University St, Montréal, Quebec, H3A 0E8, Canada
[b] Department of Geosciences, University of Tuebingen, Schnarrenbergstr. 94-96, 72076 Tuebingen, Germany
[c] Department of Earth and Atmospheric Sciences, University of Alberta, 1-26 Earth Sciences Building, Edmonton, Alberta, T6G 2E3, Canada
[d] School of Life Sciences, University of Nevada, Las Vegas, 4505 S. Maryland Pkwy., Las Vegas, NV, 89154, USA
[e] Cluster of Excellence: EXC 2124: Controlling Microbes to Fight Infection, University of Tuebingen, 72704 Tuebingen, Germany

ARTICLE INFO

Article history:
Received 18 May 2022
Received in revised form 20 January 2023
Accepted 15 February 2023
Available online xxxx
Editor: B. Wing

Keywords:
banded iron formations
trace metals
marine sediments
dissimilatory iron reducers
phytoplankton biomass
organic matter remineralization

ABSTRACT

Banded Iron Formations (BIFs) have long been considered a sedimentary record of seawater trace metal composition during the Precambrian. However, recent work has suggested that much of the trace metal composition of BIFs could have been derived from phytoplankton biomass, not seawater. In this model, phytoplankton biomass settles from the photic zone to the seafloor sediments, where it is then oxidized by heterotrophic microbes, such as dissimilatory Fe(III) reducing (DIR) bacteria, for energy generation. Remineralization of this biomass released the trace metals associated with organic molecules from phytoplankton (*i.e.*, in metalloproteins), allowing these metals to be captured by Fe oxyhydroxides and preserved in BIFs. While there is compelling evidence that the phytoplankton biomass served as a trace metal shuttle to precursor BIF sediments, it is unclear whether the degradation of biomass by DIR bacteria would liberate the biogenic trace metals as the model proposes. This work tests this hypothesis by using anoxic incubations of a model DIR bacterium (*Shewanella oneidensis* MR-1) with phytoplankton biomass as energy and carbon sources and ferrihydrite, a poorly crystalline Fe(III) oxyhydroxide ($Fe(OH)_3$), as electron acceptor. Our results show that while *S. oneidensis* MR-1 can consume some of the carbon substrates found in phytoplankton biomass, there is no evidence that *S. oneidensis* MR-1 degraded metalloproteins which would have liberated trace metals. In the context of the Precambrian, these data imply that other heterotrophic bacteria, such as fermenters, may have had a larger role in the liberation of trace metals from dead biomass during early BIF development.

1. Introduction

All life requires bioessential trace metals that act as structural components and reactive centers in metalloproteins (Jelen et al., 2016). Trends in trace metal concentrations in the sedimentary record through time reflect not only their availability in the oceans, but also their potential influence on the emergence or expansion of certain metabolisms (Robbins et al., 2016, and references therein). Over the course of Earth's history, shifts in global redox state have greatly influenced the availability of trace metals in the ocean (*e.g.*, Swanner et al., 2014). This is particularly true during the Proterozoic (2.5–0.5 Ga), where Earth's atmosphere and oceans gradually oxygenated, microbial life diversified, and eukaryotes evolved (Lyons et al., 2014).

Our understanding of trace metal contents in ancient oceans comes from various sedimentary deposits such as banded iron formations (BIFs), black shales, and authigenic pyrites (Robbins et al., 2016). Of these, BIFs are unique in that they precipitated directly out of seawater throughout the Precambrian, making them particularly useful archives to track secular changes in trace metal composition, and ultimately providing a window into the ancient marine biosphere (Konhauser et al., 2017). For example, a decline in nickel content in BIFs was used to hypothesize a "nickel famine" at ~2.7 Ga in which biogenic methane production waned, allowing for the subsequent rise in atmospheric oxygenation at around 2.45 Ga, *i.e.*, the Great Oxidation Event (GOE; Konhauser et al., 2009, 2015). In a similar manner, chromium enrichments in BIFs at 2.45 Ga were used to argue for enhanced oxidative weathering, most likely associated with the evolution of aerobic continental pyrite oxidation during the GOE (Konhauser et al., 2011). Increased oxidative weathering of land then not only supplied higher fluxes

* Corresponding author.
E-mail address: nagissa.mahmoudi@mcgill.ca (N. Mahmoudi).

https://doi.org/10.1016/j.epsl.2023.118068
0012-821X/

of critical nutrients (*e.g.*, phosphorous; Bekker and Holland, 2012) but also toxic chemical species such as arsenate that would have added a new selective pressure on the survival of marine microbial communities (Chi Fru et al., 2019).

Multiple mechanisms for BIF development have been proposed (see Bekker et al., 2014; Konhauser et al., 2017; Mänd et al., 2022 for reviews). The general consensus is that the primary precipitates were some form of ferric oxyhydroxide, such as ferrihydrite ($Fe[OH]_3$). Although there have been arguments put forth that BIF started out as a ferrous silicate, such as greenalite ($[Fe^{2+},Fe^{3+}]_{2-3}Si_2O_5[OH]_4$; Rasmussen et al., 2017), it is unlikely to have been the major contributing mineral for a number of reasons that include the implausibility that dissolved Fe(II) was not oxidized in the water column where primary productivity (*e.g.*, photoautotrophs) was present, the slightly acidic to circumneutral pH conditions of an Archean to early Paleoproterozoic ocean (Halevy and Bachan, 2017) and the low probability of basin-scale secondary oxidation through post-depositional fluids (Robbins et al., 2019). In terms of Fe(II) oxidizing mechanisms, while there is some evidence that UV photo-oxidation could have abiotically oxidized Fe(II) to Fe(III) oxyhydroxides in the Archean Eon (Anbar and Holland, 1992; Nie et al., 2017), based on rates of reaction and mass balance, photo-oxidation was not the primary mechanism for BIF precipitation (Konhauser et al., 2007). Instead, it is most likely that marine phytoplankton had critical a role in the oxidation of Fe(II) and subsequent deposition of Fe(III) oxyhydroxides (*e.g.*, ferrihydrite) that eventually formed BIFs (see Posth et al., 2013 for review).

Biological mechanisms for BIF development necessitate that ferrihydrite was precipitated in the photic zone overlying the continental shelf directly by either anoxygenic photosynthetic bacteria (the so-called photoferrotrophs) that use Fe(II) as their electron donor (Kappler et al., 2005; Posth et al., 2013), or indirectly via the abiogenic reaction of dissolved Fe^{2+} with O_2 generated by primitive cyanobacteria (Cloud, 1965; Li et al., 2021). Upon phytoplankton death, some fraction of the cellular remains would have settled through the water column to the seafloor along with the biogenic ferrihydrite. In the sediment pile, the biomass would then have undergone oxidation either during diagenesis via dissimilatory Fe(III)-reduction (DIR; as evidenced by Fe isotopes; Johnson et al., 2008) or during later metamorphism (Halama et al., 2016). Simultaneously, the ferrihydrite would have been reduced to dissolved Fe^{2+} that would have accumulated in the sediment porewaters and ultimately re-precipitated as an authigenic Fe phase, such as magnetite (Fe_3O_4), siderite ($FeCO_3$) or some form of Fe-silicate phase (Li et al., 2013a; Schad et al., 2022). The trace metals previously sorbed to the ferrihydrite would also have been solubilized and reincorporated into these authigenic mineral phases (Robbins et al., 2015).

The utility of BIFs as a paleo-marine proxy for trace metals is predicated on the notion that the precipitation of precursor ferrihydrite captured trace metals in a predictable manner based on their partitioning coefficients in seawater. This rather straightforward model, however, has generally glossed over the fact that the same phytoplankton that oxidized Fe(II) also contained a suite of trace metals in their biomass through assimilation for growth. Indeed, a recent modeling study demonstrated similarities in trace element stoichiometry (P, Mn, Co, Ni, Cu, Zn, Mo, Cd) between BIFs and photoferrotroph biomass, suggesting that phytoplankton were a major contributor to the trace elements incorporated into BIFs (Konhauser et al., 2018). Similar to the ferrihydrite, the decomposition of this phytoplankton biomass in sediments by DIR bacteria would have resulted in the release of the trace elements originally associated with biomass back into pore waters where they were captured by secondary Fe minerals (*e.g.*, magnetite, siderite) and ultimately recorded in BIFs. In summary, there likely were two major vectors for transferring metals from seawater into the sediment pile—sinking particles of ferrihydrite and dead plankton biomass—where the influence of DIR on the latter has not yet been experimentally confirmed.

A biogenic source of trace elements to BIFs puts constraints on the use of BIFs as a paleo-marine proxy for seawater chemistry. Thus, it is important to evaluate whether the microbial degradation of phytoplankton biomass would have liberated trace metals for them to be incorporated into authigenic mineral phases and preserved in BIFs. In this work, we incubated a model DIR bacterium (*Shewanella oneidensis* MR-1) under conditions that simulate Archean oceans (*i.e.*, anoxic and silica-rich) with lysed phytoplankton biomass and ferrihydrite as a proxy for biogenic Fe(III) oxyhydroxides. We collected subsamples for HCl-extractable Fe(II) and trace metal analyses to measure the reduction of Fe(III) and changes in dissolved trace metal concentrations, respectively, as *S. oneidensis* MR-1 degraded the biomass and reduced the ferrihydrite. Although photoferrotrophs are presumed to be the major contributor of biomass and thus trace metals to BIFs prior to the GOE, cyanobacteria appeared as early as in the Paleoarchean (3.6–3.3 Ga; Boden et al., 2021), and were another potential source of biomass to BIFs (Konhauser et al., 2018). Thus, we carried out parallel incubations using both photoferrotrophs and cyanobacteria as a source of phytoplankton biomass. Our results show that *S. oneidensis* MR-1 reduced Fe(III) when incubated with both photoferrotroph and cyanobacteria biomass, implying that this DIR bacterium is capable of consuming a small fraction of the carbon substrates from these biomass sources. However, trace metals associated with the biomass were not liberated into solution during this process. Thus, our broad interpretation is that the degradation of phytoplankton biomass by DIR bacteria would not have led to the release of trace metals into sediment porewaters where they could have potentially been captured by Fe minerals in the sediment and ultimately preserved in BIFs. Instead, other heterotrophic microbes would have been needed to degrade the metal-bearing compounds in phytoplankton biomass prior to the capture of these metals in precursor BIF sediments.

2. Methods

2.1. Dissimilatory Fe(III)-reducing (DIR) bacterium and culture conditions

Shewanella oneidensis MR-1 was used as a model DIR bacterial strain for this study. *S. oneidensis* MR-1 is facultative anaerobe with the capacity to reduce Fe(III) oxyhydroxides (Myers and Nealson, 1989). *S. oneidensis* MR-1 was inoculated from a frozen glycerol stock into 15 mL of liquid Luria Bertani (LB) medium (Difco #244620) and incubated aerobically at 30 °C while shaking at 140 rpm. When cultures reached an optical density at 600 nm (OD_{600}) of 0.6 to 0.8 (mid-log phase; 6 h), 500 µL of culture was transferred to 50 mL of minimal (M1) medium (Kostka and Nealson, 1998) with 20 mM lactate as the electron donor. Cultures were grown aerobically at 30 °C for 18 h while shaking at 140 rpm to an OD_{600} of 0.8 to 0.9 (late-log phase) before incubation with phytoplankton biomass.

2.2. Growth medium and ferrihydrite synthesis

Experiments were conducted using M1 basal medium with the following modifications: amorphous silica (14.21 g L^{-1} $Na_2SiO_3 \cdot 9H_2O$) was added to simulate Archean seawater silica concentrations (final concentration: 2 mM; Maliva et al., 2005), and disodium anthraquinone-2,6 disulfonate (AQDS) was added to mediate the electron transfer between *S. oneidensis* MR-1 and ferrihydrite (final concentration 0.1 mM). The final modified M1 medium

(pH 7.0) contained 3.3 mM KH_2PO_4, 5.7 mM K_2HPO_4, 9.9 µM NaCl, 45 µM H_3BO_3, 1.0 mM $MgSO_4{\cdot}7H_2O$, 0.49 mM $CaCl_2{\cdot}2H_2O$, 5.4 µM $FeSO_4{\cdot}7H_2O$, 0.11 mM L-arginine, 0.19 mM L-serine, 0.14 mM L-glutamic acid, 11.5 µM Na_2SeO_4, 2.0 mM $NaHCO_3$, 2 mM $Na_2SiO_3{\cdot}9H_2O$, and 0.1 mM AQDS.

Ferrihydrite was synthesized according to Schwertmann and Cornell (2000) using a 200 mM solution of $Fe(NO_3)_3{\cdot}9H_2O$ neutralized with 1 M KOH to a final pH of 7.5. After centrifugation of the suspension for 10 min at 5000 g (Beckman Coulter Allegra X30-R Centrifuge), the supernatant was decanted and the wet solid was washed four times (resuspended in autoclaved MilliQ water, centrifuged, and decanted) to remove excess salts. Lastly, the wet solid was resuspended in 40 mL of autoclaved MilliQ water to a final concentration of 0.5 M. The formation of poorly crystalline 2-line ferrihydrite was confirmed by X-ray diffraction (XRD) using a Proto AXRD benchtop powder X-ray diffractometer at the University of Nevada, Las Vegas.

2.3. Preparation of phytoplankton biomass

Photoferrotroph (*Chlorobium ferroxidans* strain KoFox) and cyanobacteria (*Anabaena flos-aquae* and *Synechocystis sp*. PCC 6803) biomass served as carbon substrates during incubation of *S. oneidensis* MR-1. In the ocean, phytoplankton death leads to cell lysis and release of cellular contents, such that DIR in sediments would be primarily exposed to lysed biomass (*e.g.*, Kirchman, 1999). Sonication is a commonly used laboratory method that uses sound waves to physically disrupt cell membranes and release cellular contents (*e.g.*, proteins, nucleic acids, carbohydrates, etc.) for downstream analyses. Thus, photoferrotroph and cyanobacteria biomass were placed in an ultrasonic bath for 10 min to lyse cells (as confirmed via microscopic analysis) prior to incubation with ferrihydrite and *S. oneidensis* MR-1.

C. ferrooxidans strain KoFox was cultivated on modified freshwater medium containing 0.6 g L^{-1} KH_2PO_4, 0.3 g L^{-1} NH_4Cl, 0.5 g L^{-1} $MgSO_4{\cdot}7H_2O$ and 0.1 g L^{-1} $CaCl_2{\cdot}2H_2O$ with a 22 mM bicarbonate buffer at pH 6.8-6.9 under an initial N_2/CO_2 headspace (90/10, *v*/*v*) as described in Hegler et al. (2008). The cultures were inoculated with 2% inoculum (*v*/*v*), the headspace exchanged for H_2/CO_2 (80/20, *v*/*v*) and the cultures incubated at 20 °C in light (40 W incandescent light bulb) under static conditions. The headspace was exchanged every other day to consistently provide growth substrate (H_2). Once the cultures reached stationary phase (determined by OD_{600}) they were harvested by centrifugation (7000 g), washed three times with trace metal-free M1 medium to remove any trace metals adsorbed on cell walls, and freeze-dried.

The cyanobacteria biomass used in this experiment included two model planktonic species: 63% *A. flos-aquae* and 27% *Synechocystis* sp. PCC 6803. Biomass from both cultures were combined to have sufficient material for incubations. However, given that the general macromolecular composition of cyanobacteria is similar across species (proteins > carbohydrates > lipids > nucleic acids; Finkel et al., 2016), combining biomass from these two species should not affect our results. Both cyanobacterial strains were grown in batch culture in liquid BG-11 medium (Rippka et al., 1979). Cultures were grown under cool white fluorescent lights, at 30 °C, with gentle shaking to facilitate gas exchange and prevent cells from settling to the bottom of flasks. Cultures were grown under a 16:8 h light:dark cycle, and culture density was monitored using optical density measured at 730 nm (OD_{730}). When cultures reached late log phase, cells were harvested by centrifugation at 3000 g for 5 min. Cell pellets were washed three times by resuspending in growth media and centrifuging in between washes. Cell pellets were then stored at -80°, until freeze-drying prior to incorporation in experiments.

2.4. Anoxic incubations with phytoplankton biomass

Modified M1 medium (12 mL) was aliquoted to sterile, acid-washed 25 mL glass serum bottles along with ferrihydrite (20 mM) and 12 mg of photoferrotroph or cyanobacteria biomass (42 mM organic carbon). Bottles were sealed with thick butyl rubber stoppers (Chemglass Life Sciences LLC; Vineland, NJ, USA) and crimped with aluminum seals. Subsequently, each bottle was purged with >99.998% N_2 for 15 min. The serum bottles were then injected with 240 µL of *S. oneidensis* MR-1 log phase culture (2% inoculation, *v*/*v*) using a 22-gauge needle (BD PrecisionGlide™) and 1 mL syringe. All bottles were incubated in the dark at room temperature (22 °C).

Several controls were included to track changes in Fe(III) reduction or trace metal concentrations in the absence of the *S. oneidensis* MR-1: (1) modified M1 medium, ferrihydrite, and photoferrotroph biomass; (2) modified M1 medium, ferrihydrite, cyanobacteria biomass; (3) modified M1 medium, ferrihydrite. In addition, controls with live *S. oneidensis* MR-1 in the absence of phytoplankton biomass were included to attribute any trends in Fe(III) reduction or trace metal concentrations to degradation of biomass: (1) modified M1 medium, ferrihydrite, 2% inoculation of *S. oneidensis* MR-1, and 10 mM lactate; (2) modified M1 medium, ferrihydrite, and a 2% inoculation of *S. oneidensis* MR-1 with no added carbon source. Experiments included two bottles of incubations of *S. oneidensis* MR-1 with ferrihydrite and photoferrotroph biomass, two bottles of incubations of *S. oneidensis* MR-1 with ferrihydrite and cyanobacteria biomass, and one bottle of each experimental control.

2.5. HCl-extractable Fe(II)

In the presence of ferrihydrite, *S. oneidensis* MR-1 reduces the Fe(III) oxyhydroxide and produces Fe(II), making HCl-extractable Fe(II) a reliable proxy for the activity of this isolate (Lovley et al., 1989). Daily samples were taken for HCl-extractable Fe(II) from each bottle in replicate in an anoxic chamber (95% N_2 and 5% H_2; Coy Laboratory Products, Grass Lake, MI, USA) using a 23-gauge needle (BD PrecisionGlide™) and 1 mL plastic syringe. For HCl-extractable Fe(II) analyses (measured as dissolved Fe^{2+}), 100 µL of shaken culture was extracted in replicate and placing it in 900 µL of 1 N HCl in the dark for 1 hr. Subsequently, the samples were centrifuged at 10000 rpm for 1 min, and 25 µL of supernatant was transferred into 975 µL of FerroZine reagent (buffered to pH 7.0 with 50 mM HEPES). Absorbance was measured within 5 min at 562 nm by UV-visible spectroscopy (Stookey, 1970). Iron concentrations were determined via comparison to a standard curve generated with ferrous ammonium sulfate. Reported values are an average of the two replicate measurements per bottle.

2.6. Inductively coupled plasma mass spectrometry (ICP-MS)

Changes in trace metal composition over the course of the experiment were evaluated via total dissolved trace metal concentrations. Bottles were sampled for trace metal analyses at the start (day 0), middle (day 5 for photoferrotroph biomass and day 6 for cyanobacteria biomass), and end (day 12) of each incubation. Samples were taken from each bottle in an anoxic chamber (95% N_2 and 5% H_2; Grass Lake, MI, USA) using a 23-gauge needle (BD PrecisionGlide™) and acid-washed 1 mL plastic syringe. To measure dissolved trace metal contents, sub-samples were filtered with 0.2 µm nylon filters (Basix™). All samples were placed into 4% v/v high purity HNO_3 (Optima; Fisher Scientific Company; Nepean, ON, CA) in acid-washed 15 mL polypropylene tubes. Trace metal contents were measured on a Thermo Scientific iCAP Q ICP- MS at

McGill University using yttrium as an internal standard. The instrument was calibrated with multi-element standards, and results were verified against AQUA-1 standard (National Research Council). Precision (calculated as relative standard deviation) based on the repeated analysis of standards was 1–9%, and based on technical replicates of samples was 1–5%. Reported values for incubations of *S. oneidensis* MR-1 with ferrihydrite and either photoferrotroph or cyanobacteria biomass are an average of two replicate bottles.

Total trace metal concentrations of phytoplankton biomass were measured to constrain the starting pool of metals available to *S. oneidensis* MR-1 and are reported in Supplemental Table 1. Approximately 12 mg of freeze-dried phytoplankton and cyanobacteria biomass were each digested in 69% v/v high purity HNO_3 (Optima; Fisher Scientific Company; Nepean, ON, CA) in capped 10 mL Teflon vessels (Savillex Purillex®; Eden Prairie, MN, USA) overnight (>12 h) at 120 °C. The digestant was diluted into 2% v/v high purity HNO_3 (Optima; Fisher Scientific Company; Nepean, ON, CA) in acid-washed 15 mL polypropylene tubes. For the photoferrotroph biomass, Mn, Co, Ni, Zn, and Mo were found to be above the detection limit while all other metals were below the detection limit (Supplemental Table 1). For the cyanobacteria biomass incubations, Mn, Cu, Zn, and Mo were above the detection limit (Supplemental Table 1).

While we took precautions to reduce the contribution of trace metals to our incubations (*i.e.*, acid-washing glassware, removing trace metal solutions from the M1 medium), some of the materials (*e.g.*, chemicals used to make M1 media) contained trace metals. To further constrain the background inputs of trace metals in our incubations, we measured trace metal concentrations in the modified M1 media and ferrihydrite. Modified M1 medium and 20 mM ferrihydrite were each diluted in 4% v/v high purity HNO_3 (Optima; Fisher Scientific Company; Nepean, ON, CA) in acid-washed 15 mL polypropylene tubes. The modified M1 medium and ferrihydrite had measurable concentrations of Mn and Mo, with all other metals below detection limit (Supplemental Table 1); however, these concentrations were several orders of magnitude lower than the photoferrotroph biomass (Supplemental Table 1). In contrast, the ferrihydrite had similar Mo concentrations to the cyanobacteria biomass (141 ± 0.94 nmol L^{-1} and 203 ± 90 nmol L^{-1}, respectively; Supplemental Table 1); therefore, we do not consider changes in Mo contents when evaluating incubations with cyanobacteria biomass.

3. Results

3.1. Dissimilatory Fe(III) reduction

During the 15 days of incubation of ferrihydrite (20 mM) with *S. oneidensis* MR-1 and the photoferrotroph and cyanobacterial biomass, dissolved Fe^{2+} concentrations increased to an average of 1.1 ± 0.3 mM and 1.8 ± 0.6 mM, respectively (Fig. 1). Importantly, DIR with phytoplankton biomass is significantly less than in incubations of *S. oneidensis* MR-1 and lactate (6.6 ± 0.2 mM maximum; Supplemental Fig. 1), implying that Fe(III) reduction is limited by the forms of carbon in the phytoplankton biomass. Minimal increases in Fe^{2+} (< 0.3 mM) were measured for the abiotic controls containing modified M1 medium, ferrihydrite, and either photoferrotroph or cyanobacteria biomass. Evidence of abiotic Fe(III) reduction in our experiments is not surprising given that previous work has demonstrated that organic ligands—especially humic substances—can serve as electron donors in the reduction of Fe(III) (Kappler et al., 2021). While it remains unclear which organic ligands in the phytoplankton biomass were capable of reducing ferrihydrite, several organic molecules found in biomass, such as amino acids, have been shown to reduce Fe(III) (Bhattacharyya et al., 2019). Regardless, our data imply that the increased Fe^{2+} observed during incubation of *S. oneidensis* MR-1 and biomass is primarily attributable to DIR, and hence the metabolic activity of *S. oneidensis* MR-1.

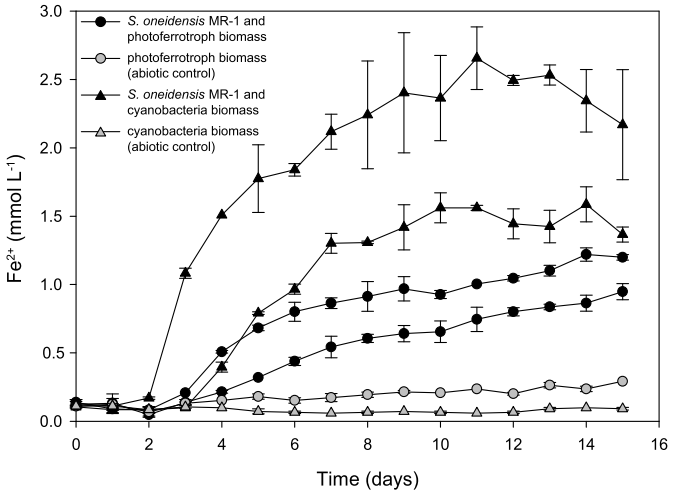

Fig. 1. Reduction of ferrihydrite (20 mM) to Fe^{2+} by *S. oneidensis* MR-1 during incubation with photoferrotroph biomass (circles; ca. 42 mM of organic carbon) and cyanobacteria biomass (triangles; ca. 42 mM of organic carbon) as a carbon source. Black symbols represent biotic replicates. Gray symbols represent abiotic controls with modified M1 medium, ferrihydrite and biomass. Data shown are the mean from duplicate measurements ± 1 standard deviation; bars not visible are smaller than the symbols.

3.2. Trace metal composition

Although we were successful in eliminating most trace metals from background sources (*e.g.*, M1 media, glassware, etc.), we anticipated that the *S. oneidensis* MR-1 cells themselves would introduce trace metals to the background pool. Thus, we measured trace metal concentrations in live controls with modified M1 medium, ferrihydrite, and a 2% inoculation of *S. oneidensis* MR-1 with no added carbon source (Figs. 2 and 3). By comparing these controls to our established background of trace metals in the modified M1 medium and ferrihydrite (Supplemental Table 1), we were able to confirm that some dissolved metals (Co, Ni, Zn, and Cu) were introduced by the inoculation of *S. oneidensis* MR-1. Therefore, trends in trace metal concentrations during incubation of *S. oneidensis* MR-1 with phytoplankton biomass were carefully considered in the context of the live control containing a 2% inoculation of *S. oneidensis* MR-1 (Figs. 2 and 3; patterned bars) and abiotic controls containing modified M1 medium, ferrihydrite, and biomass (Figs. 2 and 3; gray bars).

Characterization of the trace metals associated with the photoferrotroph biomass revealed that Mn, Co, Ni, Zn, and Mo were above the limit of detection (Supplemental Table 1), indicating that these metals were enriched in the biomass and could be potentially released during degradation of the biomass. For Mn and Zn, dissolved trace metal concentrations decreased substantially during incubation of *S. oneidensis* MR-1 with photoferrotroph biomass, suggesting no release of these metals over time. Specifically, dissolved Mn decreased by 23 ± 4 nmol L^{-1} (46% decrease; Fig. 2A), and dissolved Zn decreased by 340 ± 65 nmol L^{-1} within 12 days (100% decrease; Fig. 2B). For the other metals, such as dissolved Co (Fig. 2C) and Mo (Fig. 2D), their concentrations did not change over time and were consistent during incubation of *S. oneidensis* MR-1 with photoferrotroph biomass, as well as both the abiotic and live controls. Lastly, although a slight increase (by 39.5 ± 0.5 nmol L^{-1}; 22% increase) in dissolved Ni concentrations was observed from day 0 to 5 in bottles with *S. oneidensis* MR-1 and photoferrotroph biomass, increases were also observed in the live control (61 nmol

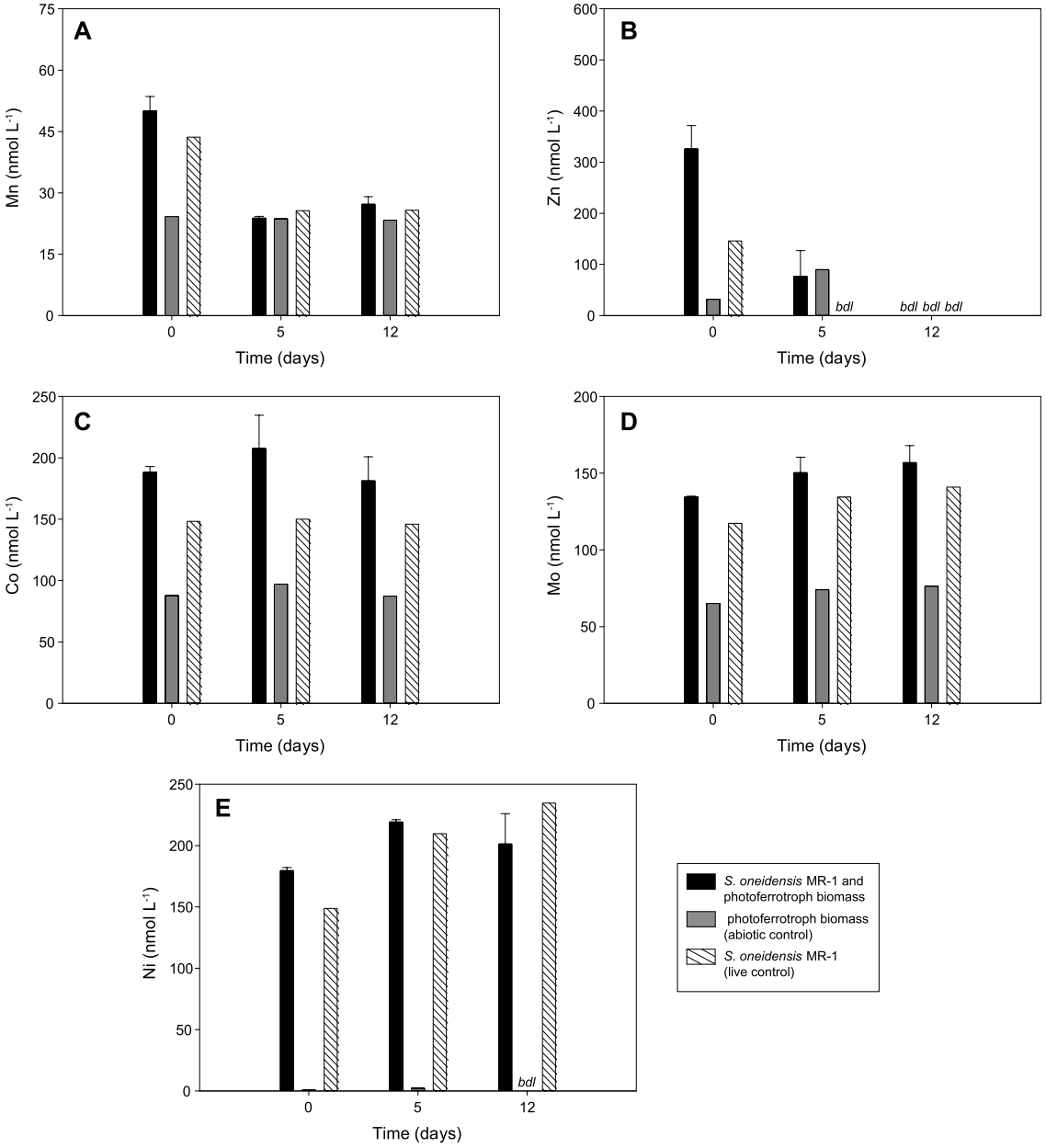

Fig. 2. Dissolved concentrations of (A) manganese, (B) zinc, (C) cobalt, (D) molybdenum, and (E) nickel for days 0, 5, and 12 during incubation of *S. oneidensis* MR-1 with photoferrotroph biomass, modified M1 medium and ferrihydrite (black bars). Data shown include an abiotic control containing modified M1 medium, ferrihydrite and photoferrotroph biomass (gray bars), and a live control containing modified M1 medium, ferrihydrite and a 2% inoculation of *S. oneidensis* MR-1 (patterned bars). For the incubations with photoferrotroph biomass and *S. oneidensis* MR-1, data are the mean from duplicate measurements ± 1 standard deviation. Data marked "*bdl*" are below the limit of detection.

L^{-1}; 41% increase; Fig. 2E), indicating that this increase is likely due to release of this metal from the *S. oneidensis* MR-1 cells as opposed to the degradation of biomass. Although there are no papers that have investigated the intracellular Ni concentrations of *S. oneidensis* MR-1, the genome for *S. oneidensis* MR-1 (Heidelberg et al., 2002) encodes for [Ni-Fe]-hydrogenase (*hyaB*). *S.oneidensis* MR-1 uses *hyaB* to catalyze the oxidation of H_2 and the reduction of the metal technetium (*e.g.*, Marshall et al., 2008; Shi et al., 2011). Therefore, a pool of intracellular Ni associated with *S. oneidensis* MR-1 cells is a plausible source of the observed increase in dissolved Ni concentrations.

For the cyanobacteria biomass, trace metal analyses showed that Mn, Cu, Zn, and Mo were above the detection limit and could be released from the biomass. However, Mo concentrations were low in the cyanobacterial biomass and comparable to background concentrations of Mo (Supplemental Table 1), thus changes in Mo were not considered during incubations with cyanobacteria biomass. Similar to incubations with photoferrotroph biomass, decreases in dissolved Mn and Zn concentrations were observed during incubation of *S. oneidensis* MR-1 with cyanobacteria biomass. Specifically, dissolved Mn and Zn concentrations decreased in bottles with *S. oneidensis* MR-1 and cyanobacteria biomass by 120 ± 16 nmol L^- (86% decrease; Fig. 3A) and 145 ± 26 nmol L^{-1} (69% decrease; Fig. 3B), respectively, over the course of the incubation. These decreases in Mn and Zn in incubations with *S. oneidensis* MR-1 and phytoplankton biomass are paralleled by similar decreases in the live control with *S. oneidensis* MR-1 and no carbon source (a 41% and 100% decrease for Mn and Zn, respectively; Fig. 3; patterned bars). There is no such trend present in incubations with biomass alone (abiotic controls; Fig. 3), implying that Mn and Zn

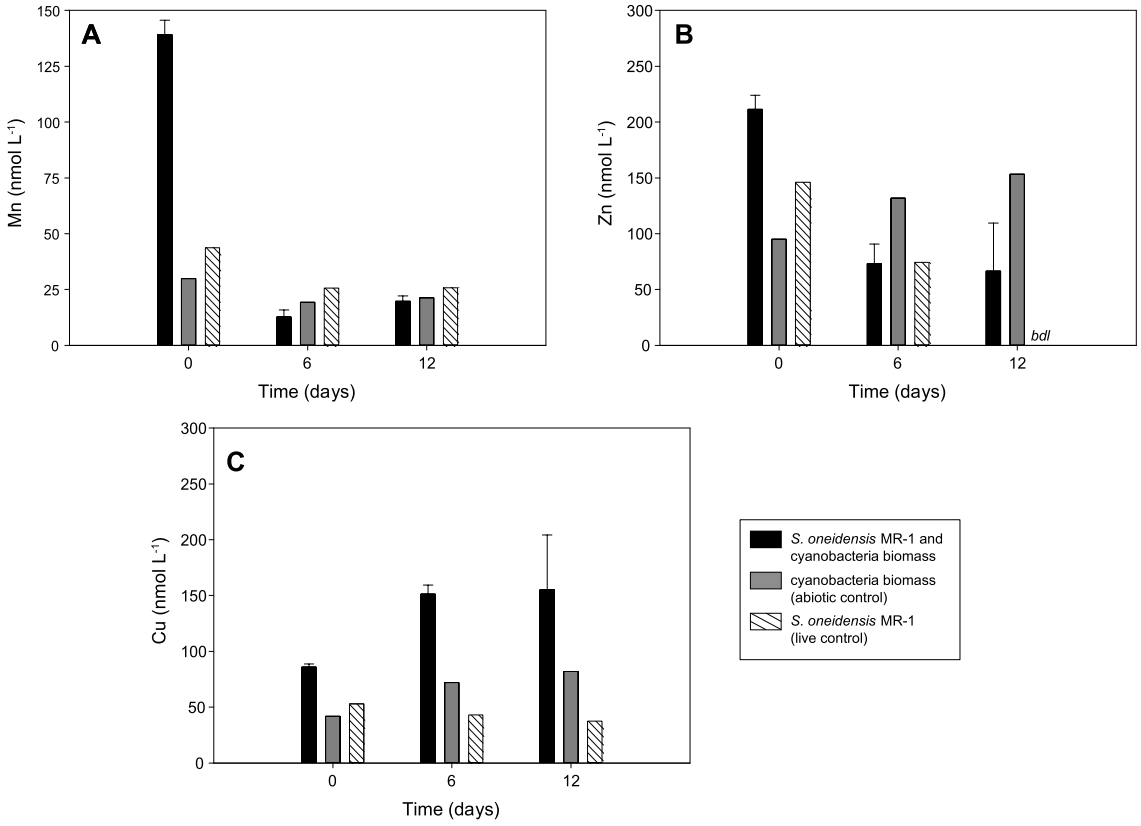

Fig. 3. Dissolved concentrations of (A) manganese, (B) zinc, and (C) copper for days 0, 6, and 12 during incubation of *S. oneidensis* MR-1 with cyanobacteria biomass, modified M1 medium and ferrihydrite (black bars). Data shown include an abiotic control containing modified M1 medium, ferrihydrite and cyanobacteria biomass (gray bars), and a live control containing modified M1 medium, ferrihydrite and a 2% inoculation of *S. oneidensis* MR-1 (patterned bars). For the incubations with cyanobacteria biomass and *S. oneidensis* MR-1, data are the mean from duplicate measurements ± 1 standard deviation. Data marked "*bdl*" are below the limit of detection. Note: the midpoint trace metal measurement for the live control (day 5) differed from the incubations with cyanobacteria biomass (day 6).

were likely removed from the dissolved phase by adsorption onto *S. oneidensis* MR-1 cell walls with and without active Fe(III) reduction.

Dissolved Cu was the only metal to have increased from days 0 to 12 (by 70 ± 26 nmol L^{-1}, 82% increase) during incubation of *S. oneidensis* MR-1 and cyanobacteria biomass (Fig. 3C; black bars). However, this trend mirrors that of the abiotic control (modified M1 media, ferrihydrite and cyanobacteria biomass), in which dissolved Cu concentrations also increased by 96% (by 40 nmol L^{-1}; Fig. 3C; gray bars). Altogether, trends in trace metal concentrations between incubations of *S. oneidensis* MR-1 with phytoplankton biomass and experimental controls suggest no discernible trend in trace metal concentration that can be attributed to the degradation of biomass by *S. oneidensis* MR-1.

It is important to note that the trace metal composition of the photoferrotroph and cyanobacteria biomass is substantially different from one another (Supplemental Table 1), likely leading to some of the differences in trace metal trends observed between incubations. For example, the cyanobacteria biomass has substantially higher Mn and Cu contents than photoferrotroph biomass. These relative enrichments could be caused by the use of these metals in oxygenic photosynthesis—Mn in the O_2-evolving complex of photosystem II and Cu in plastocyanin to aid in electron transport (Twining and Baines, 2013). Further, these trace metal compositions are different than those observed for the photoferrotroph *Rhodovulum iodosum* (as reported in Konhauser et al. (2018)). These findings are consistent with laboratory and field observations that show a vast range of the trace metal stoichiometries of phytoplankton, attributable both to environmental conditions and physiological needs (Twining and Baines, 2013).

4. Discussion

In Archean oceans, an estimated 3–15% of phytoplankton biomass from the photic zone was buried in BIF precursor sediments, although this burial rate efficiency was temporally and spatially variable (Konhauser et al., 2005; Li et al., 2013b; Thompson et al., 2019). This organic material would have been a source of energy and carbon for microbes in ancient seafloor sediments and would have driven the transformation of ferrihydrite into minerals such as magnetite and siderite (*e.g.*, Johnson et al., 2008; Konhauser et al., 2017), both major minerals in BIFs. In addition, if we assume that phytoplankton biomass served as a trace metal shuttle to sediments, microbial remineralization of biomass with ferrihydrite as the electron acceptor would have released significant quantities of trace metals back into the porewaters, eventually leading to the sequestration of these metals in precursor BIF sediments (Konhauser et al., 2018).

The Fe(III) reduction observed during our incubation experiments with phytoplankton biomass indicates that *S. oneidensis* MR-1 was able to access and consume carbon substrates needed for cellular growth and activity from both photoferrotroph and cyanobacteria biomass. However, Fe(III) reduction observed in incubations of *S. oneidensis* MR-1 with phytoplankton biomass was limited in comparison to controls with lactate. This limitation cannot be attributed to the amount of ferrihydrite present in all incubations (20 mM), nor the amount of organic carbon present (30 mM in the lactate experiments, 42 mM in the incubations with biomass). Instead, the Fe(III) reduction in our experiments must have been limited by the bioavailability of organic macromolecules present in the phytoplankton biomass. A recent estimate

compiled from 222 marine and freshwater species found that the median macromolecular composition of phytoplankton (based on dry weight) is 32% protein, 17% lipids, 15% carbohydrates, 7% nucleic acids (Finkel et al., 2016). In our incubation experiments, phytoplankton biomass was sonicated which would have lysed the cells and released some of these biomolecules into the surrounding medium. Microbes generally cannot take up these macromolecules directly, so they rely on extracellular degradative enzymes to break down these molecules to less than ~600 Da prior to uptake into the cytoplasm (Arnosti, 2011). The genome for *S. oneidensis* MR-1 has been well studied and does not encode for any known extracellular peptidases that would be required to initiate the degradation of metalloproteins (Heidelberg et al., 2002). Likewise, *S. oneidensis* MR-1 does not appear to have the metabolic capability to secrete glucosidases and lipases which would be needed to cleave complex carbohydrates and lipids, respectively, into oligomers and monomers. Interestingly, *S. oneidensis* MR-1 encodes for three different extracellular endonucleases that enable it to access nucleic acids (Gödeke et al., 2011; Heun et al., 2012). This is consistent with laboratory experiments which have demonstrated that *S oneidensis* MR-1 can consume extracellular DNA as a sole carbon and energy source under anoxic conditions (Pinchuk et al., 2008). Additional laboratory studies have shown that *S. oneidensis* MR-1 consumes simple substrates such as pyruvate (Lovley et al., 1989) and monosaccharides (Hunt et al., 2010) — both of which are found in phytoplankton cells. Although we cannot identify the specific biomolecules, it is likely that *S. oneidensis* MR-1 consumed a combination of some biomolecules as a source of carbon during our incubations. These observations are consistent with other well-known DIR bacteria found in aquatic sediments (*e.g., Geobacter metallireducens; Desulfuromonas acetoxidans; Shewanella arctica*) whose genomes do not encode for degradative enzymes; instead, they rely on small carbon substrates (Roden and Lovley, 1993; Lovley et al., 1997, and references therein; Aklujkar et al., 2009; Kim et al., 2012).

We did not observe any accumulation of dissolved trace metal concentrations in the liquid phase as a function of time, which would provide evidence that *S. oneidensis* MR-1 was degrading the metalloproteins associated with phytoplankton biomass, and subsequently liberating these trace metals. Additionally, there does not appear to be evidence of the incorporation of trace metals into *S. oneidensis* MR-1 cells during growth (*i.e.*, a decrease in dissolved trace metal content that differs from the abiotic and live controls), implying that other mechanisms caused the trends in trace metal composition in our experiments. Interestingly, trace metal concentrations in our abiotic controls did not remain constant over time (*e.g.*, Zn and Cu; incubations with cyanobacteria biomass), indicating that other processes or interactions can influence the partitioning of trace metals between dissolved and particulate (*e.g.*, ferrihydrite) fractions and would ultimately impact how trace metals are incorporated into precursor BIF sediments. Previous work examining the release of trace metals during phytoplankton decay has demonstrated that metals have different affinities for retention in biomass (*e.g.*, Co is more conservative than Zn; Hollister et al., 2020). The presence of ferrihydrite and silica in our incubations complicates our interpretations of trace metal trends even further because Fe(III) oxyhydroxides, like ferrihydrite, can strongly bind trace metals, albeit with different binding affinities for different metals (Kappler et al., 2021). Adsorption of trace metals to ferrihydrite may be stunted somewhat by amorphous silica, which binds to adsorption sites on the ferrihydrite and can outcompete other ions like phosphate, and, potentially, trace metals (Konhauser et al., 2009). Organic matter (*e.g.*, phytoplankton biomass) would also affect the extent to which metals are adsorbed to ferrihydrite, because the organic matter simultaneously competes for metal adsorption sites on the ferrihydrite while also providing additional binding sites itself (Engel et al., 2021). Thus, trace metal adsorption to ferrihydrite and dissolved phases differs when comparing metal sorption to ferrihydrite alone and metal sorption to ferrihydrite in the presence of biomass, with some metals preferentially associated with ferrihydrite (*e.g.*, Ni; Eickhoff et al., 2014), and other metals having a strong affinity for biomass (*e.g.*, Cu; Moon and Peacock, 2013). Lastly, secondary mineral phases (*e.g.*, goethite, Fe(II/III)-silicates) could have been generated during these experiments over the course of several days, attributable to the presence of Si, organic matter, and/or the reduction of ferrihydrite by DIR bacteria (Nims and Johnson, 2022; Schad et al., 2022). This, in turn, would subsequently impact the adsorption and release of trace metals from biomass and Fe minerals. Although the trace metal concentrations evaluated in this work do not provide enough resolution to identify the extent of trace metal release and adsorption to ferrihydrite, these adsorption pathways must be considered when evaluating how biogenic trace metals are incorporated into BIFs.

Our study provides a framework from which to evaluate the role of DIR in the recycling of phytoplankton biomass in precursor BIF sediments. The results strongly point to additional heterotrophic microorganisms as playing a key role in the release of trace metals associated with phytoplankton biomass back into sediment porewaters for their eventual preservation in BIFs. In modern anoxic marine sediments, organic matter is degraded through a sequence of steps with different microorganisms involved (Arndt et al., 2013). The first step is the extracellular degradation of complex macromolecules by primary degraders followed by the fermentation of oligomers and monomers to alcohols, lactate, and volatile fatty acids, which are then mineralized to CH_4, CO_2 and/or H_2. It remains unclear as to whether primary degraders and fermenters are in fact two separate populations or if fermenters are both secreting degradative enzymes and fermenting the resulting degradation products. The metabolic capability to produce extracellular enzymes is widespread across taxa (Arnosti, 2011; Zimmerman et al., 2013) and genomic reconstructions have revealed the presence of these enzymes in non-fermenting microbes (Lloyd et al., 2013). More recently, a study that investigated the anerobic degradation of organic matter in marine sediments using ^{13}C-labeled proteins and lipids found primary degraders that also encoded pathways to ferment the degradation products such as amino acids (Pelikan et al., 2021). Given that trace metals within cells are typically associated with complex proteins (*e.g.*, metalloproteins; Jelen et al., 2016), the importance of primary degraders cannot be overstated as they would have initiated the remineralization of metal-bearing compounds in phytoplankton biomass which have led to the release of trace metals back into the water column or sediment porewaters. Aside from DIR bacteria, methanogens and fermenters are thought to have been present in ancient Archean sediments (Konhauser et al., 2005; Posth et al., 2013). Regardless of whether fermenters were the primary group to initiate the degradation of macromolecules in Archean sediments, DIR bacteria would likely rely on fermenters to produce small compounds that could be readily assimilated as a carbon and energy such that the activity DIR bacteria would be limited in the absence of fermenters. Future studies focused on resolving the role and function of other heterotrophic microbes in the remineralization of phytoplankton biomass are crucial to advancing our understanding of BIFs and their function as an ancient recorder of seawater chemistry.

CRediT authorship contribution statement

Kathryn I. Rico: Investigation, Writing – original draft, Writing – review & editing. **Manuel Schad:** Investigation, Writing – review & editing. **Aude Picard:** Investigation, Writing – review & editing. **Andreas Kappler:** Investigation, Writing – review & editing. **Kurt O.**

Konhauser: Conceptualization, Writing – original draft, Writing – review & editing. **Nagissa Mahmoudi:** Conceptualization, Writing – original draft, Writing – review & editing.

Declaration of competing interest

The authors declare that they have no known competing financial interests or personal relationships that could have appeared to influence the work reported in this paper.

Data availability

Data will be made available on request.

Acknowledgements

This work was supported financially by a Wares Postdoctoral Fellowship to KR (McGill award) and a Natural Sciences & Engineering Research Council of Canada (NSERC) grant to NM (RGPIN-2019-04228) and KK (RGPIN-2020-05189). AK acknowledges infrastructural support by the Deutsche Forschungsgemeinschaft (DFG, German Research Foundation) under Germany's Excellence Strategy, cluster of Excellence EXC2124, project ID 390838134. We thank Ana Gonzalez-Nayeck (Harvard University) and Jenan Kharbush (University of Michigan) for providing cyanobacteria biomass, as well as Anna Jung (McGill) for ICP analysis and Thi Hao Bui (McGill) for technical support with anoxic incubations. We would also like to thank Jennifer Glass (Georgia Institute of Technology) and Elliott Mueller (California Institute of Technology) for thoughtful discussions that improved this study.

Appendix A. Supplementary material

Supplementary material related to this article can be found online at https://doi.org/10.1016/j.epsl.2023.118068.

References

Aklujkar, M., Krushkal, K., DiBartolo, G., Lapidus, A., Land, M.L., Lovley, D.R., 2009. The genome sequence of Geobacter metallireducens: features of metabolism, physiology and regulation common and dissimilar to Geobacter sulfurreducens. BMC Microbiol. 9, 109. https://doi.org/10.1186/1471-2180-9-109.

Anbar, A.D., Holland, H.D., 1992. The photochemistry of manganese and the origin of banded iron formations. Geochm. Cosmochim. Acta 56, 2595–2603. https://doi.org/10.1016/0016-7037(92)90346-K.

Arndt, S., Jørgensen, B.B., LaRowe, D.E., Middelburg, J.J., Pancost, R.D., Regnier, P., 2013. Quantifying the degradation of organic matter in marine sediments: a review and synthesis. Earth-Sci. Rev. 123, 53–86. https://doi.org/10.1016/j.earscirev.2013.02.008.

Arnosti, C., 2011. Microbial extracellular enzymes and the marine carbon cycle. Annu. Rev. Mar. Sci. 3, 401–425. https://doi.org/10.1146/annurev-marine-120709-142731.

Bekker, A., Holland, H.D., 2012. Oxygen overshoot and recovery during the early Paleoproterozoic. Earth Planet. Sci. Lett., 295–304. https://doi.org/10.1016/j.epsl.2011.12.012.

Bekker, A., Planavsky, N.J., Krapež, B., Rasmussen, B., Hofmann, A., Slack, J.F., Rouxel, O.J., Konhauser, K.O., 2014. Iron formation: their origins and implications for ancient seawater chemistry. In: Holland, H.D., Turekian, K.K. (Eds.), Treatise in Geochemistry, vol. 9, 2nd edition. Elsevier, Amsterdam, pp. 561–628.

Bhattacharyya, A., Schmidt, M.P., Stavitski, E., Azimzadeh, B., Martínez, C.E., 2019. Ligands representing important functional groups of natural organic matter facilitate Fe redox transformations and resulting binding environments. Geochim. Cosmochim. Acta 251, 157–175. https://doi.org/10.1016/j.gca.2019.02.027.

Boden, J.S., Konhauser, K.O., Robbins, L.J., Sánchez-Baracaldo, P., 2021. Timing the evolution of antioxidant enzymes in cyanobacteria. Nat. Commun. 12, 4742. https://doi.org/10.1038/s41467-021-24396-y.

Chi Fru, E., Somogyi, A., El Albani, A., Medjoubi, K., Aubineau, J., Robbins, L.J., Lalonde, S.V., Konhauser, K.O., 2019. The rise of oxygen-driven arsenic cycling at ca. 2.48 Ga. Geology 47, 243–246. https://doi.org/10.1130/G45676.1.

Cloud, P.E., 1965. Significance of the Gunflint (Precambrian) Microflora: photosynthetic oxygen may have had important local effects before becoming a major atmospheric gas. Science 148, 27–35. https://doi.org/10.1126/science.148.3666.27.

Eickhoff, M., Obst, M., Schröder, C., Hitchcock, A.P., Tyliszczak, T., Martinez, R.E., Robbins, L.J., Konhauser, K.O., Kappler, A., 2014. Nickel partitioning in biogenic and abiogenic ferrihydrite: the influence of silica and implications for ancient environments. Geochim. Cosmochim. Acta 140, 65–79. https://doi.org/10.1016/j.gca.2014.05.021.

Engel, M., Lezama Pacheco, J.S., Noël, V., Boye, K., Fendorf, S., 2021. Organic compounds alter the preference and rates of heavy metal adsorption on ferrihydrite. Sci. Total Environ. 750, 141485. https://doi.org/10.1016/j.scitotenv.2020.141485.

Finkel, Z.V., Follows, M.J., Liefer, J.D., Brown, C.M., Benner, I., Irwin, A.J., 2016. Phylogenetic diversity in the macromolecular composition of microalgae. PLoS ONE 11, 1–16. https://doi.org/10.1371/journal.pone.0155977.

Gödeke, J., Heun, M., Bubendorfer, S., Paul, K., Thormann, K.M., 2011. Roles of two Shewanella oneidensis MR-1 extracellular endonucleases. Appl. Environ. Microbiol. 77, 5342–5351. https://doi.org/10.1128/AEM.00643-11.

Halama, M., Swanner, E.D., Konhauser, K.O., Kappler, A., 2016. Evaluation of siderite and magnetite formation in BIFs by pressure–temperature experiments of Fe(III) minerals and microbial biomass. Earth Planet. Sci. Lett. 450, 243–253. https://doi.org/10.1016/j.epsl.2016.06.032.

Halevy, I., Bachan, A., 2017. The geologic history of seawater pH. Science 355, 1069–1071. https://doi.org/10.1126/science.aal4151.

Hegler, F., Posth, N.R., Jiang, J., Kappler, A., 2008. Physiology of phototrophic iron(II)-oxidizing bacteria: implications for modern and ancient environments. FEMS Microbiol. Ecol. 66, 250–260. https://doi.org/10.1111/j.1574-6941.2008.00592.x.

Heidelberg, J.F., Paulsen, I.T., Nelson, K.E., Gaidos, E.J., Nelson, W.C., Read, T.D., Eisen, J.A., Seshadri, R., Ward, N., Methe, B., Clayton, R.A., Meyer, T., Tsapin, A., Scott, J., Beanan, M., Brinkac, L., Daugherty, S., DeBoy, R.T., Dodson, R.J., Durkin, A.S., Haft, D.H., Kolonay, J.F., Madupu, R., Peterson, J.D., Umayam, L.A., White, O., Wolf, A.M., Vamathevan, J., Weidman, J., Impraim, M., Lee, K., Berry, K., Lee, C., Mueller, J., Khouri, H., Gill, J., Utterback, T.R., McDonald, L.A., Feldblyum, T.V., Smith, H.O., Venter, J.C., Nealson, K.H., Fraser, C.M., 2002. Genome sequence of the dissimilatory metal ion-reducing bacterium Shewanella oneidensis. Nat. Biotechnol. 20, 1118–1123. https://doi.org/10.1038/nbt749.

Heun, M., Binnenkade, L., Kreienbaum, M., Thormann, K.M., 2012. Functional specificity of extracellular nucleases of Shewanella oneidensis MR-1. Appl. Environ. Microbiol. 78, 4400–4411. https://doi.org/10.1128/AEM.07895-11.

Hollister, A.P., Kerr, M., Malki, K., Muhlbach, E., Robert, M., Tilney, C.L., Breitbart, M., Hubbard, K.A., Buck, K.N., 2020. Regeneration of macronutrients and trace metals during phytoplankton decay: an experimental study. Limnol. Oceanogr. 65, 1936–1960. https://doi.org/10.1002/lno.11429.

Hunt, K.A., Flynn, J.M., Naranjo, B., Shikhare, I.D., Gralnick, J.A., 2010. Substrate-level phosphorylation is the primary source of energy conservation during anaerobic respiration of Shewanella oneidensis strain MR-1. J. Bacteriol. 192, 3345–3351. https://doi.org/10.1128/JB.00090-10.

Jelen, B.I., Giovannelli, D., Falkowski, P.G., 2016. The role of microbial electron transfer in the coevolution of the biosphere and geosphere. Annu. Rev. Microbiol. 70, 45–62. https://doi.org/10.1146/annurev-micro-102215-095521.

Johnson, C.M., Beard, B.L., Klein, C., Beukes, N.J., Roden, E.E., 2008. Iron isotopes constrain biologic and abiologic processes in banded iron formation genesis. Geochim. Cosmochim. Acta 72, 151–169. https://doi.org/10.1016/j.gca.2007.10.013.

Kappler, A., Bryce, C., Mansor, M., Lueder, U., Byrne, J.M., Swanner, E.D., 2021. An evolving view on biogeochemical cycling of iron. Nat. Rev. Microbiol. 19, 360–374. https://doi.org/10.1038/s41579-020-00502-7.

Kappler, A., Pasquero, C., Konhauser, K.O., Newman, D.K., 2005. Deposition of banded iron formations by phototrophic Fe(II)-oxidizing bacteria. Geology 33, 865–868. https://doi.org/10.1130/G21658.1.

Kim, S.J., Park, S.J., Oh, Y.S., Lee, S.A., Shin, K.S., Roh, D.H., Rhee, S.K., 2012. Shewanella arctica sp. nov., an iron-reducing bacterium isolated from Arctic marine sediment. Int. J. Syst. Evol. Microbiol. 62, 1128–1133. https://doi.org/10.1099/ijs.0.031401-0.

Kirchman, D.L., 1999. Phytoplankton death in the sea. Nature 398, 293–294. https://doi.org/10.1038/18570.

Konhauser, K.O., Amskold, L., LaLonde, S.V., Posth, N.R., Kappler, A., Anbar, A., 2007. Decoupling photochemical Fe(II) oxidation from shallow-water BIF deposition. Earth Planet. Sci. Lett. 258, 87–100. https://doi.org/10.1016/j.epsl.2007.03.026.

Konhauser, K.O., Lalonde, S.V., Planavsky, N.J., Pecoits, E., Lyons, T.W., Mojzsis, S.J., Rouxel, O.J., Barley, M.E., Rosìere, C., Fralick, P.W., Kump, L.R., Bekker, A., 2011. Aerobic bacterial pyrite oxidation and acid rock drainage during the great oxidation event. Nature 478, 369–373. https://doi.org/10.1038/nature10511.

Konhauser, K.O., Newman, D., Kappler, A., 2005. The potential significance of microbial Fe(III) reduction during deposition of Precambrian banded iron formations. Geobiology 3, 167–177. https://doi.org/10.1111/j.1472-4669.2005.00055.x.

Konhauser, K.O., Pecoits, E., Lalonde, S.V., Papineau, D., Nisbet, E.G., Barley, M.E., Arndt, N.T., Zahnle, K., Kamber, B.S., 2009. Oceanic nickel depletion and a methanogen famine before the great oxidation event. Nature 458, 750–753. https://doi.org/10.1038/nature07858.

Konhauser, K.O., Planavsky, N.J., Hardisty, D.S., Robbins, L.J., Warchola, T.J., Haugaard, R., Lalonde, S.V., Partin, C.A., Oonk, P.B.H., Tsikos, H., Lyons, T.W., Bekker, A., Johnson, C.M., 2017. Iron formations: a global record of Neoarchaean to Palaeoproterozoic environmental history. Earth-Sci. Rev. 172, 140–177. https://doi.org/10.1016/j.earscirev.2017.06.012.

Konhauser, K.O., Robbins, L.J., Alessi, D.S., Flynn, S.L., Gingras, M.K., Martinez, R.E., Kappler, A., Swanner, E.D., Li, Y.L., Crowe, S.A., Planavsky, N.J., Reinhard, C.T., Lalonde, S.V., 2018. Phytoplankton contributions to the trace-element composition of Precambrian banded iron formations. Bull. Geol. Soc. Am. 130, 941–951. https://doi.org/10.1130/B31648.1.

Konhauser, K.O., Robbins, L.J., Pecoits, E., Peacock, C., Kappler, A., Lalonde, S.V., 2015. The Archean nickel famine revisited. Astrobiology 15, 804–815. https://doi.org/10.1089/ast.2015.1301.

Kostka, J.E., Nealson, K.H., 1998. Isolation, cultivation, and characterization of iron- and manganese-reducing bacteria. In: Burlage, R.S. (Ed.), Techniques in Microbial Ecology. Oxford University Press, Oxford, UK, pp. 58–78.

Li, W., Huberty, J., Beard, B., Valley, J., Johnson, C., 2013a. Contrasting behavior of oxygen and iron isotopes in banded iron formations as determined by in situ isotopic analysis. Earth Planet. Sci. Lett. 384, 132–143. https://doi.org/10.1016/j.epsl.2013.10.014.

Li, Y.L., Konhauser, K.O., Kappler, A., Hao, X.L., 2013b. Experimental low-grade alteration of biogenic magnetite indicates microbial involvement in generation of banded iron formations. Earth Planet. Sci. Lett. 361, 229–237. https://doi.org/10.1016/j.epsl.2012.10.025.

Li, Y., Sutherland, B.R., Gingras, M.K., Owttrim, G.W., Konhauser, K.O., 2021. A novel approach to investigate the deposition of (bio)chemical sediments: the sedimentation velocity of cyanobacteria-ferrihydrite aggregates. J. Sediment. Res. 91, 390–398. https://doi.org/10.2110/JSR.2020.114.

Lloyd, K.G., Schreiber, L., Petersen, D.G., Kjeldsen, K.U., Lever, M.A., Steen, A.D., Stepanauskas, R., Richter, M., Kleindienst, S., Lenk, S., Schramm, A., Jorgensen, B.B., 2013. Predominant archaea in marine sediments degrade detrital proteins. Nature 496, 215–218. https://doi.org/10.1038/nature12033.

Lovley, D.R., Phillips, E.J.P., Lonergan, D.J., 1989. Hydrogen and formate oxidation coupled to dissimilatory reduction of iron or manganese by Alteromonas putrefaciens. Appl. Environ. Microbiol. 55, 700–706. https://doi.org/10.1128/aem.55.3.700-706.1989.

Lovley, D.R., Coates, J.D., Saffarini, D.A., Lonergan, D.J., 1997. Dissimilatory iron reduction. In: Winkelmann, G., Carrano, C.J. (Eds.), Transition Metals in Microbial Metabolism. Hardwood Academic Publishers, Amsterdam, pp. 187–215.

Lyons, T.W., Reinhard, C.T., Planavsky, N.J., 2014. The rise of oxygen in Earth's early ocean and atmosphere. Nature 506, 307–315. https://doi.org/10.1038/nature13068.

Maliva, R.G., Knoll, A.H., Simonson, B.M., 2005. Secular change in the Precambrian silica cycle: insights from chert petrology. Bull. Geol. Soc. Am. 117, 835–845. https://doi.org/10.1130/B25555.1.

Mänd, K., Robbins, L.J., Planavsky, N.J., Bekker, A., Konhauser, K.O., 2022. Iron formations as palaeoenvironmental archives. In: Elements in Geochemical Tracers in Earth System Science. Cambridge University Press, Cambridge.

Marshall, M.J., Plymale, A.E., Kennedy, D.W., Shi, L., Wang, Z., Reed, S.B., Dohnalkova, A.C., Simonson, C.J., Liu, C., Saffarini, D.A., Romine, M.F., Zachara, J.M., Beliaev, A.S., Fredrickson, J.K., 2008. Hydrogenase- and outer membrane c-type cytochrome-facilitated reduction of technetium(VII) by Shewanella oneidensis MR-1. Environ. Microbiol. 10, 125–136. https://doi.org/10.1111/j.1462-2920.2007.01438.x.

Moon, E.M., Peacock, C.L., 2013. Modelling Cu(II) adsorption to ferrihydrite and ferrihydrite-bacteria composites: deviation from additive adsorption in the composite sorption system. Geochim. Cosmochim. Acta 104, 148–164. https://doi.org/10.1016/j.gca.2012.11.030.

Myers, C.R., Nealson, K.H., 1989. Bacterial manganese reduction and growth with manganese oxide as the sole electron acceptor. Science 4857, 1319–1321. https://doi.org/10.1126/science.240.4857.1319.

Nie, N.X., Dauphas, N., Greenwood, R.C., 2017. Iron and oxygen isotope fractionation during iron UV photo-oxidation: implications for early Earth and Mars. Earth Planet. Sci. Lett. 458, 179–191. https://doi.org/10.1016/j.epsl.2016.10.035.

Nims, C., Johnson, J.E., 2022. Exploring the secondary mineral products generated by microbial iron respiration in Archean ocean simulations. Geobiology 20, 743–763. https://doi.org/10.1111/gbi.12523.

Pelikan, C., Wasmund, K., Glombitza, C., Hausmann, B., Herbold, C.W., Flieder, M., Loy, A., 2021. Anaerobic bacterial degradation of protein and lipid macromolecules in subarctic marine sediment. ISME J. 15 (3), 833–847. https://doi.org/10.1038/s41396-020-00817-6.

Pinchuk, G.E., Ammons, C., Culley, D.E., Li, S.M.W., McLean, J.S., Romine, M.F., Nealson, K.H., Fredrickson, J.K., Beliaev, A.S., 2008. Utilization of DNA as a sole source of phosphorus, carbon, and energy by Shewanella spp.: ecological and physiological implications for dissimilatory metal reduction. Appl. Environ. Microbiol. 74, 1198–1208. https://doi.org/10.1128/AEM.02026-07.

Posth, N.R., Konhauser, K.O., Kappler, A., 2013. Microbiological processes in banded iron formation deposition. Sedimentology 60, 1733–1754. https://doi.org/10.1111/sed.12051.

Rasmussen, B., Muhling, J.R., Suvorova, A., Krapež, B., 2017. Greenalite precipitation linked to the deposition of banded iron formations downslope from a late Archean carbonate platform. Precambrian Res. 290, 49–62. https://doi.org/10.1016/j.precamres.2016.12.005.

Rippka, R., Deruelles, J., Waterbury, J.B., 1979. Generic assignments, strain histories and properties of pure cultures of cyanobacteria. J. Gen. Microbiol. 111, 1–61. https://doi.org/10.1099/00221287-111-1-1.

Robbins, L.J., Funk, S.P., Flynn, S.L., Warchola, T.J., Li, Z., Lalonde, S.V., Rostron, B.J., Smith, A.J.B., Beukes, N.J., de Kock, M.O., Heaman, L.M., Alessi, D.S., Konhauser, K.O., 2019. Hydrogeological constraints on the formation of Palaeoproterozoic banded iron formations. Nat. Geosci. 12, 558–563. https://doi.org/10.1038/s41561-019-0372-0.

Robbins, L.J., Lalonde, S.V., Planavsky, N.J., Partin, C.A., Reinhard, C.T., Kendall, B., Scott, C., Hardisty, D.S., Gill, B.C., Alessi, D.S., Dupont, C.L., Saito, M.A., Crowe, S.A., Poulton, S.W., Bekker, A., Lyons, T.W., Konhauser, K.O., 2016. Trace elements at the intersection of marine biological and geochemical evolution. Earth-Sci. Rev. 163, 323–348. https://doi.org/10.1016/j.earscirev.2016.10.013.

Robbins, L.J., Swanner, E.D., Lalonde, S.V., Eickhoff, M., Paranich, M.L., Reinhard, C.T., Peacock, C.L., Kappler, A., Konhauser, K.O., 2015. Limited Zn and Ni mobility during simulated iron formation diagenesis. Chem. Geol. 402, 30–39. https://doi.org/10.1016/j.chemgeo.2015.02.037.

Roden, E.E., Lovley, D.R., 1993. Dissimilatory Fe (III) reduction by the marine microorganism Desulfuromonas acetoxidans. Appl. Environ. Microbiol. 59, 734–742. https://doi.org/10.1128/aem.59.3.734-742.1993.

Schad, M., Byrne, J.M., ThomasArrigo, L.K., Kretzschmar, R., Konhauser, K.O., Kappler, A., 2022. Microbial Fe cycling in a simulated Precambrian ocean environment: Implications for secondary mineral (trans)formation and deposition during BIF genesis. Geochim. Cosmochim. Acta 331, 165–191. https://doi.org/10.1016/j.gca.2022.05.016.

Schwertmann, U., Cornell, R.M., 2000. Iron Oxides in the Laboratory: Preparation and Characterization. WILEY_VHC, Weinheim, Germany.

Shi, L., Belchik, S.M., Plymale, A.E., Heald, S., Dohnalkova, A.C., Sybirna, K., Bottin, H., Squier, T.C., Zachara, J.M., Fredrickson, J.K., 2011. Purification and characterization of the [NiFe]-hydrogenase of Shewanella oneidensis MR-1. Appl. Environ. Microbiol. 77, 5584–5590. https://doi.org/10.1128/AEM.00260-11.

Stookey, L.L., 1970. Ferrozine-a new spectrophotometric reagent for iron. Anal. Chem. 42, 779–781. https://doi.org/10.1021/ac60289a016.

Swanner, E.D., Planavsky, N.J., Lalonde, S.V., Robbins, L.J., Bekker, A., Rouxel, O.J., Saito, M.A., Kappler, A., Mojzsis, S.J., Konhauser, K.O., 2014. Cobalt and marine redox evolution. Earth Planet. Sci. Lett. 390, 253–263. https://doi.org/10.1016/j.epsl.2014.01.001.

Thompson, K.J., Kenward, P.A., Bauer, K.W., Warchola, T., Gauger, T., Martinez, R., Simister, R.L., Michiels, C.C., Llirós, M., Reinhard, C.T., Kappler, A., 2019. Photoferrotrophy, deposition of banded iron formations, and methane production in Archean oceans. Sci. Adv. 5, 1–9. https://doi.org/10.1126/sciadv.aav2869.

Twining, B.S., Baines, S.B., 2013. The trace metal composition of marine phytoplankton. Annu. Rev. Mar. Sci. 5, 191–215. https://doi.org/10.1146/annurev-marine-121211-17232.

Zimmerman, A.E., Martiny, A.C., Allison, S.D., 2013. Microdiversity of extracellular enzyme genes among sequenced prokaryotic genomes. ISME J. 7, 1187–1199. https://doi.org/10.1038/ismej.2012.176.